Modeling the fragmentation patterns of triacylglycerides in mass spectrometry allows the quantification of the regioisomers with a minimal number of standards

David Balgoma, Yann Guitton, Jason J. Evans, Bruno Le Bizec, Gaud Dervilly-Pinel, Anne Meynier

Modeling the Fragmentation Patterns of Triacylglycerides in Mass Spectrometry Allows the Quantification of the Regioisomers with a Minimal Number of Standards

Balgoma, David[1,2*]; Guitton, Yann[2]; Evans, Jason J.[3]; Le Bizec, Bruno[2]; Dervilly-Pinel, Gaud[2]; Meynier, Anne[1]

[1]UR1268 BIA (Biopolymères Interactions Assemblages), INRA, 44316, Nantes

[2]Laberca, Oniris, INRA, Université Bretagne Loire, 44307, Nantes-France

[3]Chemistry Department, University of Massachusetts Boston, Boston, MA 02125

***Corresponding author**

David Balgoma,
david.balgoma-hernando@inra.fr, dbalgoma@gmail.com
Biopolymères Interactions Assemblages
Equipe Interfaces et Systèmes Dispersés
Institut National de la Recherche Agronomique
3, Impasse Yvette Cauchois
La Géraudière
CS 71627
44316 NANTES CEDEX 3 - France

***Corresponding author present address**

david.balgoma@ilk.uu.se
Institutionen för Läkemedelskemi
Biomedicinskt Centrum
Uppsala Universitet
Husargatan 3
753 21 Uppsala
Sweden

Abstract

Mass spectrometry allows the relative quantification of the regioisomers of triacylglycerides by the calibration of their fragmentation patterns. However, due to the plethora of regioisomers of triacylglycerides, calibration with every standard is not feasible. An analytical challenge in the field is the prediction of the fragmentation patterns of triacylglycerides to quantify their regioisomers. Thus, we aimed to model these fragmentation patterns to quantify the regioisomeric composition, even for those without commercially available standards. In a first step, we modeled the fragmentation patterns of the regioisomers of triacylglycerides obtained from different published datasets. We found the same qualitative trends of fragmentation beyond differences in the type of adduct in these datasets (both $[M+NH_4]^+$ and $[M+H]^+$), and the type of instrument (orbitrap, Q-ToF, ion-trap, single quadrupole, and triple quadrupole). However, the quantitative trends of fragmentation were adduct and instrument specific. From these observations, we modeled quantitatively the common trends of fragmentation of triacylglycerides in every dataset. In a second step, we applied this methodology on a Synapt G2S Q-ToF to quantify the regioisomers of triacylglycerides in sunflower and olive oils. The results of our quantification were in good agreement with previous published quantifications of triacylglycerides, even for regioisomers that were not present in the training dataset. The species with more than two highly unsaturated fatty acids (arachidonic, eicosapentaenoic, and docosahexaenoic acids) showed a complex behavior and lower predictability of their fragmentation patterns. However, this framework presents the capacity to model this behavior when more data are available. It would be also applicable to standardize the quantification of the regioisomers of triacylglycerides in an inter-laboratory ring study.

Keywords: triacylglycerols, positional isomers, regioisomers, lipidomics, modeling.

Abbreviations

AA, arachidonic acid; ALA, α-linoleic acid; APCI, atmospheric pressure chemical ionization, Ar, arachidic acid; B, behenic acid; CID, collision induced dissociation; DHA, docosahexaenoic acid; EPA, eicosapentaenoic acid; ESI, electrospray ionization; GLA, γ-linolenic acid; L, linoleic acid; La, lauric acid; M, myristic acid; Mo, myristoleic acid; O, oleic acid; MU, monounsaturated; P, palmitic acid; Po, palmitoleic acid; PUFA, polyunsaturated fatty acids; S, stearic acid; SM, supplementary material; SP, structural parameter; SV, structural vector; TG, triacylglyceride; UHPLC-MS, ultrahigh performance liquid chromatography hyphenated to mass spectrometry.

1. Introduction

Triacylglycerides (TGs) are key components of foodstuffs because of their impact on their physical, textural, sensory, and nutritional properties. TGs also constitute the main daily source of dietary fatty acids (close to 90%), which play a key role in different physiological processes, such as energetic metabolism, cell structure, and innate immunity [1,2]. To achieve their physiological role, dietary lipids and constitutive fatty acids have to be digested. During this process in the gastrointestinal tract, gastric lipase in the stomach first hydrolyzes the TGs, which releases the fatty acids in the *sn*-3 position of the glycerol backbone. Subsequently, pancreatic lipase in the small intestine hydrolyzes the *sn*-1 and *sn*-3 positions. These successive reactions yield mainly free fatty acids from the *sn*-1 and *sn*-3 positions. The fatty acids in the *sn*-2 position yield mainly 2-acylglycerol (Figure 1A). Consequently, the regioisomeric composition of TGs – *i.e.* the relative composition of the fatty acids at the *sn*-2 position of TGs– conditions how the fatty acids are absorbed. This different absorption affects the nutrition characteristics of dietary fats in foodstuffs. As classical example, when palmitic acid is esterified in the *sn*-1 and *sn*-3 positions of TGs in infant formulas, it is released during digestion as free palmitate. It interacts with calcium ions to form and insoluble soap that is excreted in feces. Consequently, palmitic acid in this type of formulas is not available as source of energy for the infant [3]. In addition, eicosapentaenoic acid (EPA) and docosahexaenoic acid (DHA) are more efficiently absorbed and redistributed in tissues when they are esterified in the *sn*-2 position of the dietary TGs [4,5]. EPA and DHA play a key role in inflammation as precursors of pro-resolving lipid mediators [6]. This is one of the rationales behind the recommendation of ingestion of fish oils with ω-3 fatty acids to prevent cardiovascular diseases. However, due to the enzyme specificity during the digestion, fish oils with different regioisomeric composition may have different effects on cardiovascular risks. In summary, the

quantification of the regioisomers of TGs in fish oils may have a direct impact on public health [7].

Traditionally, TG regioisomers have been determined by enzymatic hydrolysis and the subsequent characterization of the products by liquid, thin layer, or gas chromatography [8–11]; but this procedure is cumbersome. In addition, silver-ion chromatography separates TG regioisomers, but it is not high-throughput [8,12]. On the contrary, lipidomics enables the high-throughput study of lipids in complex samples, even with quantitative approaches [13]. Specifically, lipidomics already plays a key role in food authentication [14] and in new approaches to precision nutrition [15–17]. State-of-the-art lipidomics uses ultrahigh performance liquid chromatography hyphenated to mass spectrometry (UHPLC-MS), which allows the identification of the lipids under collision induced dissociation [18–21]. In mass spectrometry, TGs ionize in electrospray (ESI) as adducts of single charged cations [22] ($[M+Cation]^+$ with Cation=Li^+, Na^+, K^+, or NH_4^+) or in atmospheric pressure chemical ionization (APCI) as $[M+H]^+$. Both $[M+NH_4]^+$ and $[M+H]^+$ adducts suffer neutral losses of the fatty acids to yield diacylglycerol-like ions [23,24] (Figure 1B). From a structural point of view, the MS^2 fragmentation tendency of a fatty acid in a TG depends on the type of adduct, on the position of the fatty acid, on the structure of the fatty acid, and on the influence of the other fatty acids esterified to the glycerol backbone (interaction term). On the other hand, MS^2 fragmentation does not allow for the fatty acids in the *sn*-1 and *sn*-3 positions to be distinguished. Because of this reason, the *sn*-1 and *sn*-3 positions are usually called *external* positions, and the *sn*-2 position is called *internal* position. Pioneering studies in the fragmentation of TGs proposed mechanisms of reaction to explain the fragmentation patterns for TGs with saturated and monounsaturated fatty acids [25–28]. They reported a higher tendency of the fatty acids to be lost in the external positions when compared with the internal position, which has been studied by

computational chemistry [29]. Nevertheless, mass spectrometry lacks of reproducibility and the fragmentation patterns of molecules depend on the specific instrument. By calibrating the relative abundance of the neutral losses of the fatty acids of a TG in a specific instrument, the regioisomeric composition can be quantified [30]. In the literature, this calibration is restricted to species with two different fatty acids without constraints. This calibration uses simple linear regression and can yield quantifications of the regioisomers below 0%, above 100%, or with the sum of the regioisomers different from 100%.

By using fragmentation patterns in mass spectrometry, we aimed to quantify the regioisomeric composition of TGs. Up to date, this quantification faces three main challenges: A) the application of multivariate constrained calibration to species with three different fatty acids; B) the calibration for every regioisomer of TGs in complex samples is not feasible; and C) the MS^2 fragmentation patterns are instrument specific. Here we address these three challenges and report a model to quantify the regioisomeric composition of TGs in the context of lipidomics. To achieve these aims, we hypothesized that there are fragmentation patterns of available TGs can be used to predict the fragmentation of non-available TGs. Consequently, 1) we applied the multivariate constrained calibration to the quantification of the regioisomers of TGs; 2) we studied the influence of the fragmentation energy on the fragmentation patterns of TGs; 3) we analyzed qualitatively the fragmentation patterns of the regioisomers of TGs in published datasets; 4) we modeled the identified fragmentation patterns in terms of the position of the fatty acids, the structure of the fatty acids, and the interaction among the fatty acids; and 5) we quantified the regioisomers of TGs in vegetable oils with a limited number of standards.

2. Materials and methods

2.1. Notation of the TGs, of the quantification of their regioisomers, and of their fragmentation patterns.

For a TG with three fatty acids A, B and C, the notation TG(A/B/C) expressed the three possible regioisomers, which were represented as TG(rac-B/A/C), TG(rac-A/B/C), and TG(rac-A/C/B). The prefix rac- differed from the prefix *sn*- to denote a combination of enantiomers, which cannot be distinguished by fragmentation in mass spectrometry. Consequently, the relative quantification of the regioisomers TG(rac-B/A/C), TG(rac-A/B/C), and TG(rac-A/C/B) was defined as the percentage of the internal position esterified with, respectively, the fatty acids A, B, and C.

The structure of a TG affects the relative abundance of the neutral losses of the fatty acids under fragmentation by collision induced dissociation (CID) [26]. We defined a structural parameter (SP) as the logarithm of the ratios of the signals of the neutral loses of two fatty acids, corrected by their multiplicity in the TG (Equation 1). These structural parameters compare the relative tend of two fatty acids to suffer neutral loss in a pure regioisomer or a mixture of regioisomers. We also defined the structural vectors (SV) to organize these structural parameters for the pure regioisomers and the mixtures of regioisomers. In a TG with three different fatty acids (A, B, and C), the structural vector possessed three different structural parameters that expressed mathematically the fragmentation patterns (Equation 2). Under the assumption of linear behavior, we considered the structure vector of a mixture as the linear combination of the structure vectors of the pure regioisomers (Equation 3). The regioisomeric composition of the mixture is, by definition, the coefficients of this linear combination (α_i, for the possible pure regioisomers i in Equation 3). As the quantification of the regioisomers must be in the interval [0%, 100%], we constrained these coefficients to avoid negative values,

quantifications above 100%, and quantifications of regioisomers that do not sum 100%. Full development of the equations for the different multiplicities of fatty acids and an illustrative example for the regioisomers of TG(P/O/L) are provided in SM-B.

2.2. Datasets to characterize, model, and quantify the regioisomers of TGs

To build fragmentation models, only the TGs containing common fatty acids of vegetable or fish oils were selected: lauric acid (La), myristic acid (M), palmitic acid (P), stearic acid (S), arachidic acid (Ar), behenic acid (B), myristoleic acid (Mo), palmitoleic acid (Po), oleic acid (O), linoleic acid (L), α-linolenic acid (ALA), γ-linolenic acid (GLA), arachidonic acid (AA), EPA, or DHA. The structural vectors of the datasets selected are provided in SM-A.

The Boston dataset contained the fragmentation data of regioisomers of TGs ionized in ESI as $[M+NH_4]^+$ adducts were acquired on a ThermoFinnigan LCQ Advantage ion-trap mass spectrometer with ESI (Sunnyvale, CA) at the University of Massachusetts Boston [31–34]. The fragmentations were performed at relative collision energy of 30 (unitless scale). Calibration curves for the regioisomers of TG(rac-O/S/O)-TG(rac-S/O/O); TG(rac-S/O/S)-TG(rac-S/S/O); and TG(rac-P/S/O)-TG(rac-S/P/O)-TG(rac-P/O/S) were also acquired at the University of Massachusetts Boston.

The Pardubice dataset contained regioisomers of TGs with P, S, O, L, ALA, and GLA that were ionized by APCI as $[M+H]^+$ in five different instruments: orbitrap, Q-ToF, ion-trap, single quadrupole, and triple quadrupole [35]. In all five instruments the $[M+H]^+$ adduct fragmented spontaneously to suffer the neutral loss of the fatty acids.

The Nantes dataset was built by using the regioisomers TG(rac-P/O/P), TG(rac-P/P/O), TG(rac-P/L/P), TG(rac-S/P/O), TG(rac-O/P/O), TG(rac-O/O/P), TG(rac-P/L/S), TG(rac-P/O/L), TG(rac-L/L/P), TG(rac-M/O/B), TG(rac-O/L/O), TG(rac-O/O/L),

TG(rac-L/S/L), TG(rac-L/O/L), TG(rac-L/L/O), TG(rac-O/O/ALA), and TG(rac-L/L/GLA) purchased from Larodan, Solna, Sweden. The regioisomers were analyzed on an Acquity-Synapt G2S Q-ToF (Waters). The standards and oils were separated on a BEH C18 2.1x150 mm (Waters) by a 16-minute gradient of solvents: A) methanol, 2 mM ammonium acetate, 6 mM acetic acid; and B) methanol/isopropanol 50:50, 2 mM ammonium acetate, 6 mM acetic acid. The chromatographic system did not separate the regioisomers of TGs but partially separated TGs with the same number of carbons and unsaturations to obtain spectra without interferences (*e.g.* TG(52:2) in Figures S-1 and S-2). The analytes were ionized by ESI in positive mode and yielded the adduct $[M+NH_4]^+$. After optimization (see Section 3.2), the fragmentations were carried out in the trap at 13 V of energy of fragmentation. The signals of the fragments were corrected by the isotopic distribution of the diacylglycerol-like ions [35].

2.3. Software and statistics

Data analysis and model development were performed in R 3.3.1 run under RStudio 0.99.902. The optimization of the fragmentation parameters was carried out with function *optim* from package *stats* (Nelder-Mead method, minimization of the sum of squares of the prediction of the measured structural vectors). The multivariate constrained regression to quantify the regioisomers was carried out by the function *pcls* from package *mgcv* [36]. In all cases log stands for natural logarithm. The deviation of the quantification of the regioisomers was expressed by the bias. As the sum of the abundance of the possible regioisomers is necessarily 100%, the values are linearly dependent and the differences between the quantification and the reference values is always zero. To avoid this effect, the bias was defined as the absolute value of the difference between the measured regioisomeric composition and the prepared regioisomeric composition (in-house

reference material). Outliers were detected by Dixon's Q test. Comparisons were analyzed by differences-average plots [37].

All molecules were drawn in MarvinSketch 15.9.7.0 and figures were processed in GIMP 2.8.16.

3. Results and Discussion

3.1. Quantification of the regioisomers by multivariate constrained regression. Interpolation among pure standards

To avoid senseless calibrations of the regioisomeric composition we used multivariate regression with constraints according to Equations 1, 2, and 3 (further details in SM-B). To study the error of the multivariate constrained calibration we used at least 10 different mixtures of regioisomers of TG(rac-O/S/O)-TG(rac-S/O/O); of TG(rac-S/O/S)-TG(rac-S/S/O); and of TG(rac-P/S/O)-TG(rac-S/P/O)-TG(rac-P/O/S), which were acquired at the same conditions as the Boston dataset. The matrices of regression were fitted by minimum of squares, which yielded the average of the biases below 5% (minimum sum of squares column in Table 1). While previous publications had quantified TGs with two different fatty acids, our methodology was also suitable for species with three different fatty acids. In comparison with previous studies, our methodology also avoided the quantification of the relative abundance of the regioisomers with values below 0%, above 100%, and with sum of the possible regioisomers different from 100%.

On the other hand, by knowing the extremes of the calibration –*i.e.* the structural vectors of the pure regioisomers– we could estimate the matrix of regression (an example of the calculations can be found in SM-B5). This substitution assumed a linear relationship in the regression. In this case, the average of the bias of the quantification was slightly higher for the three types of mixtures, but below 5% in all cases (Table 1). In conclusion, the characterization of the fragmentation patterns of the regioisomers of TGs allowed the quantification of mixtures by interpolation. The underlying assumption

is the linear relationship between the regioisomeric composition and the structural vectors.

3.2. Influence of the energy of fragmentation on the fragmentation patterns represented by the structural vectors.

To study the specific impact of the fragmentation energy on the structural vectors, we modified this parameter during the fragmentation of the TGs constituting the Nantes dataset. In this case, the fragmentation was performed on a Synapt G2S Q-ToF by CID of the $[M+NH_4]^+$ adducts (parent ion). All standards showed three types of fragments: 1) $[M+H]^+$ ions by neutral loss of ammonia (minor peak); 2) diacylglycerol-like ions by the neutral losses of the fatty acids (predominant at low energy of fragmentation); and 3) $[\text{fatty acid-CO}]^+$ and $[\text{fatty acid-CO+74}]^+$ ions (predominant at high energy of fragmentation). Previous studies have suggested that these ions are generated sequentially in three steps: 1^{st}) neutral loss of ammonia from $[M+NH_4]^+$ to yield the $[M+H]^+$ ion (primary fragment), 2^{nd}) neutral loss of the fatty acids from $[M+H]^+$ to yield the diacylglycerol-like ions (secondary fragments), and 3^{rd}) further dissociation of the diacylgycerol-like ions to yield the $[\text{fatty acid-CO}]^+$ and $[\text{fatty acid-CO+74}]^+$ ions (tertiary fragments) [26,38]. As the relative abundance of the diacylglycerol-like ions (secondary fragments) contains the structural information that we aim to model to quantify the regioisomers, we center the discussion about the factors that govern the generation of these ions. The signal of these secondary fragments presented a wide maximum in relation to the energy of fragmentation (*e.g.* TG(rac-POL) in Figure 2A). However, the changes were not proportional for the neutral losses, which affected the structural parameters (Figure 2B). Considering this behavior, the signal of the secondary fragments depended on two reactions: 1) the reaction of production by the neutral loss

of the fatty acids from the primary fragment, and 2) the reactions of consumption to yield the tertiary fragments. At low energy of fragmentation, the production overrode the consumption; situation that changed gradually by increasing the energy of fragmentation until they were equal at the maximum. At high energy of fragmentation, the consumption overrode the production and the signals of the secondary fragments disappeared (Figure 2A). From a structural point of view, the reaction of production depended on the structure of the parent ion –this structure was what we aimed to model in attempt to quantify the regioisomers. However, the reactions of consumption of the secondary fragments were not directly related to the structure of the parent ion, but to the structure of the secondary fragments [26]. Consequently, the presence of tertiary fragments hampered the possibility of modeling the fragmentation patterns of TGs from their structure. These tertiary fragments must be minimized to relate the patterns of fragmentation into the primary ions to the structure of the parent ion (and, hence, the regioisomeric composition). Considering this factors, we chose an energy of fragmentation of 13 V in the Nantes dataset. At this energy of fragmentation, the production of the secondary fragments dominated their signal and there were no tertiary fragments. We will discuss in detail the mechanism of fragmentation in different instruments and adducts in Section 3.4, after the identification and modeling of the fragmentation patterns in the datasets.

In conclusion, to model the fragmentation patterns of the regioisomers in different instruments, the neutral losses of the fatty acids of TGs should be the main mechanism of fragmentation (*i.e.* the secondary fragments should not decompose into tertiary fragments). This behavior is expected to take place at low energy of fragmentation. As the energy transfer and the type of adduct are instrument-specific, the fragmentation conditions should be optimized on every instrument as described before.

3.3. Identification of the qualitative fragmentation patterns of pure regioisomers of TGs when ionized as $[M+NH_4]^+$ in ESI and $[M+H]^+$ in APCI. Influence of the type of analyzer and adduct on the fragmentation patterns from a qualitative point of view.

To identify trends in the neutral losses of fatty acids in TGs as $[M+NH_4]^+$ adduct in ESI, we analyzed qualitatively the datasets from Boston [31–34] and from Nantes. To study the trends of fragmentation of TGs ionized as $[M+H]^+$ adduct in APCI, we analyzed qualitatively the Pardubice dataset [35]. By exploratory data analysis of the structural parameters (SM-A), we found four patterns of TG fragmentation in CID to yield the neutral loss of the fatty acids:

I. Species with only saturated fatty acids. A) The structural parameters comparing two saturated fatty acids in external positions were close to zero. This behavior indicates that the number of carbons showed a minor influence in the patterns of fragmentation [19]. B) The structural parameters comparing a saturated fatty acid in the internal position and a saturated fatty acid in the external position were lower than zero. This behavior indicates a higher trend of saturated fatty acids to be lost in the external position, which agrees with previous results [29].

II. Species with saturated and mono-unsaturated fatty acids with an unsaturation cis in position 9 (Mo, Po and O). When compared with a saturated fatty acid, the monounsaturated fatty acids showed a higher tendency to be lost in both the external and the internal positions. When a TG species had three monounsaturated fatty acids, the structural parameters depended only on the position of the fatty acid (in this case, the structural parameters were close to those of a TG with three saturated species, *e.g.* TG(rac-Mo/O/Mo) and TG(rac-P/S/P) in SM-A). This behavior indicates

that the fragmentation tendencies in these TGs depended only on the position and the type of fatty acid. Consequently, there is no interaction term in these TGs.

III. Species with one polyunsaturated fatty acid (PUFA, *i.e.* L, ALA, GLA, AA, EPA, or DHA). When compared with saturated and monounsaturated fatty acids, the tendency of PUFAs to suffer a neutral loss correlated positively with the number of unsaturations. All other factors equal, the tendency to be lost was higher when the first unsaturation was closer to the carboxylic group (*e.g.* GLA *vs* ALA, SM-A). This behavior suggests the introduction of a fragmentation parameter for every PUFA in the fragmentation models.

IV. Species with two or three PUFAs. When there were more than one PUFA, they presented lower differences in the structural parameters than expected. For example, under the assumption of independence of the fragmentation of fatty acids, the structural parameter between palmitic acid and linoleic acid in TG(rac-S/P/L) was expected to be similar to TG(rac-L/P/L). Nevertheless, in the first case the value was -1.34 while in the second one it was, on average, 0.13 (SM-A, Boston dataset). As PUFAs show a globular-like structure, we attribute this behavior to an interaction among PUFAs *via* intramolecular London dispersion forces. These forces would be weaker for species with saturated fatty acids, which present a linear structure. As the neutral loss of these PUFAs is inhibited, these forces would increase the energy of the transition state of the reaction of fragmentation. From a modeling point of view, this behavior suggests the introduction of a fragmentation parameter for the inhibition of the neutral loss of PUFAs when more than one PUFA is present in the TG species.

If we compare the ionization type in the three datasets, the $[M+H]^+$ adduct in APCI (Pardubice dataset) showed the same qualitative fragmentation patterns as the

$[M+NH_4]^+$ adduct in ESI, but the quantitative values differed. For example, $SP_{P/O}$ in TG(rac-P/O/P) was, on average, 0.89 for the adduct $[M+NH_4]^+$ in the Boston dataset, while the value was 0.99 in the Nantes dataset (SM-A). On the other hand this structural parameter was, on average, 0.57 for the adduct $[M+H]^+$ in the Pardubice dataset (SM-A). Consequently, the neutral loss of P was favored over O in the three datasets for TG(rac-P/O/P), but the degree of this difference depended on the instrument and adduct. These facts point to the existence of homogeneous qualitative trends of fragmentation in the three datasets. However, the quantitative trends were adduct and instrument specific. Further comparisons among adducts and instruments are provided in the next Section, after modeling these fragmentation patterns.

3.4. Modeling the fragmentation patterns of TGs: assumptions and comparison of the fragmentation models among adducts and instruments

To predict the fragmentation patterns of the regioisomers of TGs by the structural vectors, we modeled the structural parameters as differences of the tendency of the fatty acids to suffer a neutral loss. These tendencies were quantified by the parameters Γ for a fatty acid in a specific regioisomer. These parameters eventually depended on the ratios of the rate constants of the neutral losses, considered as reactions in competition [38]. To relate the parameters Γ with the structure, the parameter Γ of a fatty acid was modeled as a sum of the fragmentation parameters γ. The fragmentation parameters γ depended on 1) the position of the fatty acid in the glycerol backbone, 2) the structure of the fatty acid, and 3) the interaction among fatty acid chains.

Consequently, we modeled the fragmentation tendencies of the fatty acids by the fragmentation parameters γ according to the trend groups identified in Section 3.3: A)

γ_{ext} for the external position; B) γ_{MU} for monounsaturated fatty acids with the double bond in position 9 (Mo, Po, O); C) γ_{L}, γ_{ALA}, γ_{GLA}, γ_{EPA}, and γ_{DHA} for respective PUFAs; and D) γ_{IN} for the interaction among PUFAs. As the model was based on the differences of the parameters Γ, the origin of the scale was fixed for the saturated fatty acids in the internal position (*i.e.* $\Gamma_{sat,int}$, γ_{int}, and γ_{sat} equaled zero). Formulae and further details can be found in SM-C. The fitted fragmentation parameters γ reproduced and quantified the trends observed in Section 3.3 (Table 2). All other factors equal: 1) the loss of an external fatty acid was favored in comparison with the internal fatty acids ($\gamma_{ext} < 0$); 2) the neutral loss of a fatty acid increased with the number of unsaturations and the closer the position of the first unsaturation was to the carboxylic group (γ_{MU}, γ_{L}, γ_{ALA}, and γ_{GLA}, in all datasets with also γ_{EPA}, and γ_{DHA} in the Boston dataset); and 3) the presence of more than one PUFA inhibited the tendency of a PUFA to suffer a neutral loss ($\gamma_{IN} > 0$). Regarding model repeatability, the relative standard deviation of the parameters γ_{ext}, γ_{MU}, γ_{L}, γ_{ALA}, γ_{GLA}, and γ_{IN} was, respectively, 2.8, 5.4, 2.5, 5.7, 2.5, and 5.2% (four batches in the Nantes dataset). Consequently, despite the difference among adducts and instruments (Table 2), the fragmentation model showed good repeatability for the same instrument.

To test the capacity of quantification of the regioisomers of TGs by the model, we compared the quantification bias of the regioisomers of TG(S/O/O), TG(S/S/O), and TG(P/S/O) in the Boston dataset with the quantification by multivariate constrained regression (Section 3.1). First, we predicted the structural vectors by the γ parameters in Table 2 for the Boston dataset as in SM-C. Subsequently we used these vectors as the columns of the regression matrix to apply the multivariate constrained regression as in SM-B. The average of the quantification bias by using the model was below 10% in all cases (right column in Table 1). In comparison with the quantifications without

non-modeled structural vectors, the bias was higher for the regioisomers of TG(S/O/O) and TG(S/S/O), but lower for the regioisomers of TG(P/S/O) (Table 1, last column). In conclusion, despite a moderate increase of the error, the bias below 10% was also acceptable to use the model to quantify the regioisomers of TGs.

The complexity of the fragmentation of PUFAs affected the quality of the prediction, specifically in species with highly unsaturated fatty acids (AA, EPA, and DHA) when another PUFA was present in the TG. For example, $SP_{O/AA}$ in TG(rac-O/AA/L) in the Boston dataset was -0.80 while the model predicted 0.49 (SM-A). We address this lack of predictability to a simplification in modeling the interaction between PUFAs into only one parameter. Most of the species in the Boston dataset with more than one highly unsaturated fatty acids were of the form TG(rac-A/B/A) whereas the interaction *via* London dispersion forces between the highly unsaturated fatty acids could be different in the regioisomer TG(rac-A/A/B). Consequently, we speculate that the interaction between highly unsaturated fatty acids depended on the structure of the fatty acids and their relative position in the glycerol backbone. Considering that these species corresponded to the adduct $[M+NH_4]^+$, we also speculate that the hydrogens of the ammonia and the folded structure of the highly unsaturated fatty acids interact *via* hydrogen bonds to produce complex fragmentation patterns. This factor would be absent in adducts without this effect, such as $[M+Li]^+$ or $[M+Na]^+$. In summary, this complex behavior warrants further research to understand and model the fragmentation patterns of different adducts of TGs with highly unsaturated fatty acids [39]. Specifically, this research is necessary to allow the quantification of the regioisomers of TGs in fish oils or derived products, such as oils enriched in DHA and EPA (accounting for more than 50% of the fatty acids in these oils).

Comparing adducts and instruments in the datasets under study, the fragmentation parameters (γ_{ext}, γ_{MU}, γ_{L}, γ_{ALA}, γ_{GLA}, and γ_{IN}) showed the same sign but different absolute value. This behavior of the fragmentation parameters was the mathematical expression of the observation of common qualitative trends of fragmentation for the adducts and modes of ionization (Section 3.3). However, this behavior cannot be extrapolated to other adducts, as discussed later.

Considering the same adduct in different instruments, we can first compare the behavior of the $[M+NH_4]^+$ adducts in the Nantes and Boston datasets. On the one hand, the Nantes dataset was acquired by CID in a Q-ToF at low energy of fragmentation to prevent the presence of tertiary fragments (see Section 3.2). On the other hand, the Boston dataset was acquired on an ion-trap analyzer with CID energy of fragmentation of 30 (unitless scale) without the presence of tertiary fragments. CID fragmentations in both Q-ToF and ion-trap are classified as low energy activation and the energy transferred is vibrational [40]. However, we observed tertiary fragments in the Nantes dataset at high energy of fragmentation, but not in the Boston dataset. This fact points to a higher transfer of energy on the Q-ToF system, at least when compared to the ion-trap. At low energy of fragmentation in the Q-ToF, the energy transferred would be sufficient to excite the vibrational states of the ester groups of the fatty acids of TGs to yield their neutral loss of the fatty acids (secondary fragments). However, it would not be enough to excite the vibrational states of the functional groups of these secondary fragments to yield the tertiary fragments. Consequently, at low energy of fragmentation, we would expect the same mechanism of fragmentation by CID on the ion-trap in the Boston dataset and on the Q-ToF in the Nantes dataset. Another potential difference in the fragmentation process during CID is the gas of collision. In CID, the collisions with a noble gas convert the translational energy of the ion into

internal energy, including the vibrational states. In this process, the heavier the collision gas, the higher the transfer of energy [40]. In this context, we would not expect to change the mechanism of fragmentation by changing the gas of collision, only the degree of dissociation would change. In conclusion and despite the differences in the analyzers, we expected the same mechanism of fragmentation of the $[M+NH_4]^+$ adducts in the Nantes and Boston datasets. This justifies the presence of the same qualitative fragmentation patterns for the two datasets. We address the differences in the quantitative patterns among instruments to: 1) the differences in energy transfer to the analytes during both the ionization and the fragmentation, and 2) the different time-range between fragmentation and detection for Q-ToF and ion-trap instruments.

We can also compare the fragmentation trends for the $[M+H]^+$ adducts on the five instruments in the Pardubice dataset. In this case, the regioisomers of TGs fragmented spontaneously in APCI from the $[M+H]^+$ adduct and did not report the presence of tertiary fragments in any of the five analyzers [35]. As TGs are thermolabile, we address the fragmentation to thermal decomposition during the ionization and/or the ion transfer in the mass spectrometers. Despite the differences in the analyzers, thermal energy is also transferred to the vibrational states of the molecule. Thus, we would expect the same mechanism of fragmentation among the five analyzers used in the Pardubice dataset. This common mechanism justifies the same qualitative fragmentation patterns for the $[M+H]^+$ adducts in APCI in these five analyzers. In a similar way, we address the differences in the quantitative patterns to the differences in energy transfer to the analytes during both the ionization (*e.g.* differences in the temperature of ionization [35]).

Considering different adducts, we could expect differences even in the qualitative trends of fragmentation. These differences would originate in putative qualitative differences in the vibrational states of the different parent ions. In last term, these differences would be linked to the different interaction between the analyte and the cation, which would affect the structure of the parent ion in gas phase. As discussed in Section 3.2, the neutral losses of the fatty acids for the adduct $[M+NH_4]^+$ in ESI originated from the fragment $[M+H]^+$. Despite we observed the same qualitative trends of fragmentation for the $[M+NH_4]^+$ adduct in ESI and $[M+H]^+$ adduct in APCI, we cannot assume that the structure of the parent ion $[M+H]^+$ in APCI is the same as the primary fragment $[M+H]^+$ from $[M+NH_4]^+$ in ESI. From a general point of view, other adducts (*e.g.* $[M+Li]^+$, $[M+Na]^+$, or $[M+Ag]^+$) also present an inhibition of the neutral loss of the fatty acids in the internal position of the glycerol [22,25]. However, the type of cation could affect the intramolecular London forces and, consequently, the other qualitative fragmentation patterns described in Section 3.3.

3.5. Quantification of the regioisomers of TGs in vegetable oils by using a Synapt G2S Q-ToF instrument

3.5.1. Assumptions of the quantification by interpolation of the fragmentation patterns of pure regioisomers

Two underlying assumptions should be studied on a specific instrument to apply this quantification: 1) the linearity of the response, and 2) the equal efficiency of fragmentation for the regioisomers. We studied these two assumptions for the adduct $[M+NH_4]^+$ on a Synapt G2S Q-ToF fragmenting at 13 V of energy in the trap.

Regarding linearity, we injected four types of mixtures of regioisomers and we obtained a linear relationship (*e.g.* the pair TG(rac-O/P/O) and TG(rac-O/O/P) in Figure 3).

Regarding the efficiency of fragmentation, we studied the sum of the signal of the neutral losses normalized by the signal of the parent ion (Table 3). Our results reproduced those previously published for the $[M+H]^+$ adduct [41]. The number of carbons (C) and the number of unsaturations (U) of a TG species explained the variation in the efficiency of fragmentation by the equation log(Efficiency)= -4.1-0.054C-0.20U (error of the fitting in Figure S-3). Consequently, for coeluting species with the same number of carbons and unsaturations, we reconstructed the signal of the common fatty acids in proportion. Subsequently, the regioisomeric composition was calculated by using the reconstructed spectra.

3.5.2. Quantification of the regioisomers in vegetable oils

After ensuring the underlying assumptions of the model, we predicted the regression matrices of the different regioisomers from the fragmentation parameters γ_{ext}, γ_{MU}, γ_{L}, γ_{ALA}, γ_{GLA}, and γ_{IN} in the Nantes dataset (Table 2). An illustrative example of the calculations can be found in SM-C6. As the samples were vegetable oils, we considered that all fatty acids with 18 carbons and 3 unsaturations were ALA, which cannot be distinguished from GLA by the mass of their neutral loss. The absences of GLA was verified by gas chromatography analysis of the fatty acids (data not shown). No species contained highly unsaturated fatty acids, which are not present in vegetable oils.

We compared our quantification and the previously reported values for these oils (Table 4, Figure S-4). As example of a TG with all regioisomers in the training

dataset, we can consider the quantification of the regioisomers of TG(O/O/P) in both sunflower and olive oils. In both cases, our quantification yielded the pure regioisomer TG(rac-O/O/P). This quantification agrees previous studies, which had reported an abundance of this regioisomer of at least 91% in sunflower oil, and 95% in olive oil. As example of a TG without any regioisomer in the training dataset, we can consider the quantification of the regioisomers of TG(S/O/L) in sunflower oil. In this case, our quantification yielded a composition of 42% of TG(rac-S/O/L), 58% of TG(S/L/O), and 0% of TG(rac-O/S/L). A previous study by chemical deacylation reported a composition of, respectively, 45%, 55%, and 0%, which is in good agreement [11]. For a broader comparison beyond specific examples, we used the difference-average plot (Figure S-4). This plot did not show systematic deviations by type of regioisomer, amount of regioisomer, and type of oil. The average of the independent differences was -1.4% and the standard deviation was 17%. Considering the interval of confidence, only one measurement was out (95% of confidence in Figure S-4). This point corresponded to the regioisomers of TG(S/S/L) in sunflower oil. TG(S/S/L) partially coeluted with TG(O/O/S), being, respectively, approximately 3% and 97% of the peak. In the spectrum of fragmentation of TG(S/S/L) there was a minor contribution of TG(O/O/S), which affected the quantification of the regioisomeric composition. After discarding this outlier (Dixon's Q test p-value $< 2.2\ 10^{-16}$), the average of the differences was 1.2% and the standard deviation 11%. In addition, the species present in the training dataset did not show differences with the species not present in the training dataset (Figure S-4).

4. Conclusions

In this study, we describe a framework to quantify the regioisomeric composition of TGs by modeling their mass spectrometry fragmentation. This methodology was applicable even for species of TGs that were not included in the training dataset. To achieve this aim, we enclosed the structural information of the TGs in the fragmentation parameters γ. These parameters predicted the tendency of a fatty acid to suffer a neutral loss, which were considered as reactions in competition. The fragmentation parameters γ presented the same sign for the different adducts and instruments in the studied datasets. This behavior suggests the existence of common fragmentation mechanism and the use of a common model predict the fragmentation patterns of TGs in different instruments. However, the fragmentation parameters γ presented different absolute values for the different adducts and instruments in the studied datasets. This behavior suggests the necessity of fitting the common model for every instrument.

After the study of the assumptions of the model, the quantification of the regioisomers of TGs in vegetable oils was in good agreement with previous results, even for regioisomers that were not present in the training dataset. As limitation, the fragmentation patterns of TGs with more than one highly unsaturated fatty acids were too complex to be modeled with the up-to-date data. However, after description of these patterns, this framework presents the capability of predicting the fragmentation patterns of these TGs, which are the main components of fish oils.

As an interesting perspective to this work, an inter-laboratory ring study may establish a universal minimal set of standards of TGs to model their fragmentation patterns. The TGs with highly unsaturated fatty acids would be of special interest in this ring study. In addition, this ring study may establish: 1) the ionization and fragmentation conditions in

different instruments to homogenize the quantitative fragmentation patterns, and 2) a full validation of the quantification of regioisomers of TGs. This full validation would be achieved by the quantification of the regioisomers of TGs in fish and vegetable oils by both reference enzymatic methods and the framework we present in this study.

In conclusion and despite the transitory limitation for TGs with highly unsaturated fatty acids, this framework opens the quantification of all regioisomers of TGs by using a minimal number of standards in high-throughput lipidomics.

5. Appendix A. Supplementary Materials

The datasets from Boston, Pardubice, and Nantes are provided in SM-A. The mathematical expression of the fragmentation patterns for the quantification of regioisomers by multivariate constrained regression is provided in SM-B. The description and formulae of modeling the fragmentation patterns of the TGs are described in SM-C. Supplementary figures can be found in SM-D.

Acknowledgements

We thank Michelle Viau, Karinne Pouponneau, and Fabrice Monteau for expert technical assistance and advice. We also thank Prof. Michal Holčapek for providing guidance about the fragmentation patterns reported in the Pardubice dataset. We also thank Dr. Carlos Palo-Nieto for advice in the discussion of the reactivity of the TGs in gas phase.

Funding

The authors are grateful to the Région Pays de la Loire, France (Grant RFI Cap Aliment– Food for Tomorrow – AlDOL)

Conflict of Interest Discloser

The authors declare no conflict of interest

References

[1] G. van Meer, D.R. Voelker, G.W. Feigenson, Membrane lipids: where they are and how they behave, Nat. Rev. Mol. Cell Biol. 9 (2008) 112–124.

[2] C.D. Funk, Prostaglandins and leukotrienes: advances in eicosanoid biology, Science 294 (2001) 1871–1875.

[3] M. Ramírez, L. Amate, A. Gil, Absorption and distribution of dietary fatty acids from different sources, Early Hum. Dev. 65 Suppl (2001) S95–S101.

[4] H. Sadou, C.L. Léger, B. Descomps, J.N. Barjon, L. Monnier, A. Crastes de Paulet, Differential incorporation of fish-oil eicosapentaenoate and docosahexaenoate into lipids of lipoprotein fractions as related to their glyceryl esterification: a short-term (postprandial) and long-term study in healthy humans, Am. J. Clin. Nutr. 62 (1995) 1193–1200.

[5] M.S. Christensen, C.E. Høy, C.C. Becker, T.G. Redgrave, Intestinal absorption and lymphatic transport of eicosapentaenoic (EPA), docosahexaenoic (DHA), and decanoic acids: dependence on intramolecular triacylglycerol structure, Am. J. Clin. Nutr. 61 (1995) 56–61.

[6] E.A. Dennis, P.C. Norris, Eicosanoid storm in infection and inflammation, Nat. Rev. Immunol. 15 (2015) 511–523.

[7] H. Iso, M. Kobayashi, J. Ishihara, S. Sasaki, K. Okada, Y. Kita, Y. Kokubo, S. Tsugane, JPHC Study Group, Intake of fish and n3 fatty acids and risk of coronary heart disease among Japanese: the Japan Public Health Center-Based (JPHC) Study Cohort I, Circulation 113 (2006) 195–202.

[8] T. Řezanka, K. Pádrová, K. Sigler, Regioisomeric and enantiomeric analysis of triacylglycerols, Anal. Biochem. 524 (2017) 3–12.

[9] M. Lísa, M. Holčapek, Characterization of triacylglycerol enantiomers using chiral HPLC/APCI-MS and synthesis of enantiomeric triacylglycerols, Anal. Chem. 85 (2013) 1852–1859.

[10] S.E. Hancock, B.L.J. Poad, A. Batarseh, S.K. Abbott, T.W. Mitchell, Advances and unresolved challenges in the structural characterization of isomeric lipids, Anal. Biochem. 524 (2017) 45–55.

[11] V.P. Pchelkin, E.I. Kuznetsova, V.D. Tsydendambaev, A.G. Vereshchagin, Determination of the Positional-Species Composition of Plant Reserve Triacylglycerols by Partial Chemical Deacylation, Russ. J. Plant Physiol. 48 (2001) 701–707.

[12] M. Lísa, H. Velínská, M. Holcapek, Regioisomeric characterization of triacylglycerols using silver-ion HPLC/MS and randomization synthesis of standards, Anal. Chem. 81 (2009) 3903–3910.

[13] M. Li, E. Baughman, M.R. Roth, X. Han, R. Welti, X. Wang, Quantitative profiling and pattern analysis of triacylglycerol species in Arabidopsis seeds by electrospray ionization mass spectrometry, Plant J. Cell Mol. Biol. 77 (2014) 160–172.

[14] J.M. Bosque-Sendra, L. Cuadros-Rodríguez, C. Ruiz-Samblás, A.P. de la Mata, Combining chromatography and chemometrics for the characterization and authentication of fats and oils from triacylglycerol compositional data-a review, Anal. Chim. Acta. 724 (2012) 1–11.

[15] G. Astarita, J. Langridge, An emerging role for metabolomics in nutrition science, J. Nutr. Nutr. 6 (2013) 181–200.

[16] J.T. Smilowitz, A.M. Zivkovic, Y.-J.Y. Wan, S.M. Watkins, M.L. Nording, B.D. Hammock, J.B. German, Nutritional lipidomics: molecular metabolism, analytics, and diagnostics, Mol. Nutr. Food Res. 57 (2013) 1319–1335.

[17] F.H. Chilton, R. Dutta, L.M. Reynolds, S. Sergeant, R.A. Mathias, M.C. Seeds, Precision Nutrition and Omega-3 Polyunsaturated Fatty Acids: A Case for Personalized Supplementation Approaches for the Prevention and Management of Human Diseases, Nutrients 9 (2017).
[18] S.S. Bird, V.R. Marur, M.J. Sniatynski, H.K. Greenberg, B.S. Kristal, Serum lipidomics profiling using LC-MS and high-energy collisional dissociation fragmentation: focus on triglyceride detection and characterization, Anal. Chem. 83 (2011) 6648–6657.
[19] K. Nagy, L. Sandoz, F. Destaillats, O. Schafer, Mapping the regioisomeric distribution of fatty acids in triacylglycerols by hybrid mass spectrometry, J. Lipid Res. 54 (2013) 290–305.
[20] Y.H. Rustam, G.E. Reid, Analytical Challenges and Recent Advances in Mass Spectrometry Based Lipidomics, Anal. Chem. 90 (2018) 374–397.
[21] J. La Nasa, I. Degano, L. Brandolini, F. Modugno, I. Bonaduce, A novel HPLC-ESI-Q-ToF approach for the determination of fatty acids and acylglycerols in food samples, Anal. Chim. Acta. 1013 (2018) 98–109.
[22] L.C. Herrera, M.A. Potvin, J.E. Melanson, Quantitative analysis of positional isomers of triacylglycerols via electrospray ionization tandem mass spectrometry of sodiated adducts, Rapid Commun. Mass Spectrom. 24 (2010) 2745–2752.
[23] E. Hvattum, Analysis of triacylglycerols with non-aqueous reversed-phase liquid chromatography and positive ion electrospray tandem mass spectrometry, Rapid Commun. Mass Spectrom. 15 (2001) 187–190.
[24] P. Laakso, P. Voutilainen, Analysis of triacylglycerols by silver-ion high-performance liquid chromatography-atmospheric pressure chemical ionization mass spectrometry, Lipids 31 (1996) 1311–1322.
[25] F.F. Hsu, J. Turk, Structural characterization of triacylglycerols as lithiated adducts by electrospray ionization mass spectrometry using low-energy collisionally activated dissociation on a triple stage quadrupole instrument, J. Am. Soc. Mass Spectrom. 10 (1999) 587–599.
[26] A.M. McAnoy, C.C. Wu, R.C. Murphy, Direct qualitative analysis of triacylglycerols by electrospray mass spectrometry using a linear ion trap, J. Am. Soc. Mass Spectrom. 16 (2005) 1498–1509.
[27] C. Cheng, M.L. Gross, E. Pittenauer, Complete structural elucidation of triacylglycerols by tandem sector mass spectrometry, Anal. Chem. 70 (1998) 4417–4426.
[28] W.M. Lauer, A.J. Aasen, G. Graff, R.T. Holman, Mass spectrometry of triglycerides. 1. Structural effects, Lipids 5 (1970) 861–868.
[29] J.S. Grossert, L. Cubero Herrera, L. Ramaley, J.E. Melanson, Studying the chemistry of cationized triacylglycerols using electrospray ionization mass spectrometry and density functional theory computations, J. Am. Soc. Mass Spectrom. 25 (2014) 1421–1440.
[30] J. Cvacka, E. Krafková, P. Jiros, I. Valterová, Computer-assisted interpretation of atmospheric pressure chemical ionization mass spectra of triacylglycerols, Rapid Commun. Mass Spectrom. 20 (2006) 3586–3594.
[31] M. Malone, J.J. Evans, Determining the relative amounts of positional isomers in complex mixtures of triglycerides using reversed-phase high-performance liquid chromatography-tandem mass spectrometry, Lipids 39 (2004) 273–284.
[32] X. Li, J.J. Evans, Examining the collision-induced decomposition spectra of ammoniated triglycerides as a function of fatty acid chain length and degree of unsaturation. I. The OXO/YOY series, Rapid Commun. Mass Spectrom. 19 (2005) 2528–2538.
[33] X. Li, E.J. Collins, J.J. Evans, Examining the collision-induced decomposition spectra of ammoniated triglycerides as a function of fatty acid chain length and degree of

unsaturation. II. The PXP/YPY series, Rapid Commun. Mass Spectrom. 20 (2006) 171–177.
[34] R. Gakwaya, X. Li, Y.L. Wong, S. Chivukula, E.J. Collins, J.J. Evans, Examining the collision-induced decomposition spectra of ammoniated triglycerides. III. The linoleate and arachidonate series, Rapid Commun. Mass Spectrom. 21 (2007) 3262–3268.
[35] M. Holčapek, H. Dvořáková, M. Lísa, A.J. Girón, P. Sandra, J. Cvačka, Regioisomeric analysis of triacylglycerols using silver-ion liquid chromatography-atmospheric pressure chemical ionization mass spectrometry: comparison of five different mass analyzers, J. Chromatogr. A. 1217 (2010) 8186–8194.
[36] S.N. Wood, Fast stable restricted maximum likelihood and marginal likelihood estimation of semiparametric generalized linear models: Estimation of Semiparametric Generalized Linear Models, J. R. Stat. Soc. Ser. B Stat. Methodol. 73 (2011) 3–36.
[37] J.M. Bland, D.G. Altman, Comparing methods of measurement: why plotting difference against standard method is misleading, Lancet Lond. Engl. 346 (1995) 1085–1087.
[38] J.B. Renaud, S. Overton, P.M. Mayer, Energy and entropy at play in competitive dissociations: The case of uneven positional dissociation of ionized triacylglycerides, Int. J. Mass Spectrom. 352 (2013) 77–86.
[39] E.J. Judge, D. Zheng, S. Chivukula, R. Gakwaya, S. Schostarez, X. Li, M. Liriano, J.J. Evans, A simple and economical strategy for obtaining calibration plots for relative quantification of positional isomers of YYX/YXY triglycerides using high-performance liquid chromatography/tandem mass spectrometry, Rapid Commun. Mass Spectrom. 31 (2017) 1690–1698.
[40] E. de Hoffmann, V. Stroobant, Mass spectrometry: principles and applications, third edition, J. Wiley, Chichester, West Sussex, England; Hoboken, NJ, 2007.
[41] W.C. Byrdwell, Critical Ratios for structural analysis of triacylglycerols using mass spectrometry, Lipid Technol. 27 (2015) 258–261.
[42] M. Lísa, H. Velínská, M. Holcapek, Regioisomeric characterization of triacylglycerols using silver-ion HPLC/MS and randomization synthesis of standards, Anal. Chem. 81 (2009) 3903–3910.
[43] J.-T. Lin, A. Arcinas, Analysis of regiospecific triacylglycerols by electrospray ionization-mass spectrometry(3) of lithiated adducts, J. Agric. Food Chem. 56 (2008) 4909–4915.
[44] A. Jakab, I. Jablonkai, E. Forgács, Quantification of the ratio of positional isomer dilinoleoyl-oleoyl glycerols in vegetable oils, Rapid Commun. Mass Spectrom. 17 (2003) 2295–2302.
[45] H.M. Leskinen, J.-P. Suomela, H.P. Kallio, Quantification of triacylglycerol regioisomers by ultra-high-performance liquid chromatography and ammonia negative ion atmospheric pressure chemical ionization tandem mass spectrometry, Rapid Commun. Mass Spectrom. 24 (2010) 1–5.

Figure 1. Structure and fragmentation of TGs. A) Structure of TG(*sn*-16:0/18:1/18:2). The fatty acids esterified in the *sn*-1 or *sn*-3 positions are collectively known as external fatty acids; the fatty acid esterified in the *sn*-2 position is known as internal fatty acid. B) Fragmentation pattern of the regioisomer TG(rac-16:0/18:1/18:2) at low energy of fragmentation (13 V on a Synapt G2S Q-ToF). No tertiary fragments were detected at this energy of fragmentation.

Figure 2. Influence of the fragmentation energy on the signal of the neutral losses and the structural parameters of the adduct $[M+NH_4]^+$ on a Synapt G2S Q-ToF. A) Logarithm of the signal (arbitrary units, AU) of the parent ion of TG(rac-P/O/L) and the neutral losses (NL) of NH_3 and the fatty acids as a function of the energy of fragmentation. B) Structural parameters (SP) of TG(rac-P/O/L) as a function of the energy of fragmentation.

Figure 3. Response of the structural parameters to the regioisomeric composition. Linear response of the structural parameter between oleic and palmitic acids ($SP_{O/P}$) for mixtures of TG(rac-O/O/P) and TG(rac-O/P/O). The adduct $[M+NH_4]^+$ was fragmented on a Synapt G2S Q-ToF at 13V of fragmentation energy (R^2=0.99).

Figure 1

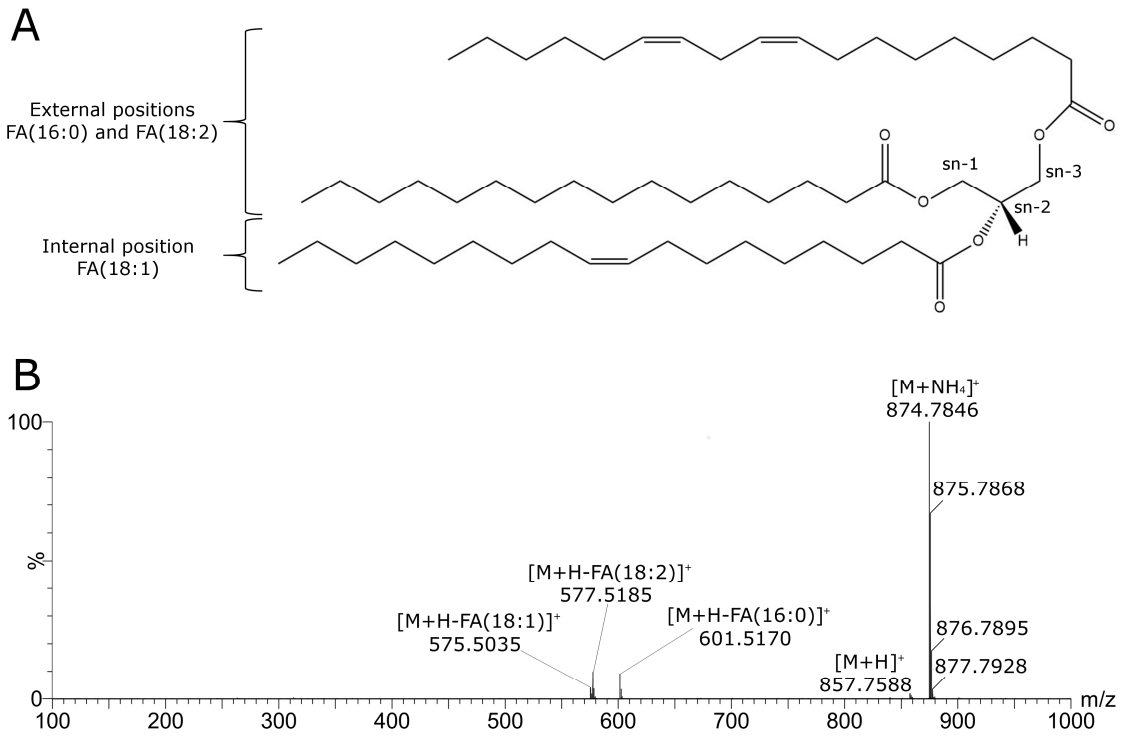
A
External positions
FA(16:0) and FA(18:2)
Internal position
FA(18:1)
sn-1
sn-2
sn-3
H
B
100
%
0
[M+NH4]+
874.7846
875.7868
[M+H-FA(18:2)]+
577.5185
[M+H-FA(18:1)]+
575.5035
[M+H-FA(16:0)]+
601.5170
876.7895
[M+H]+
857.7588
877.7928
100
200
300
400
500
600
700
800
900
1000
m/z

Figure 2

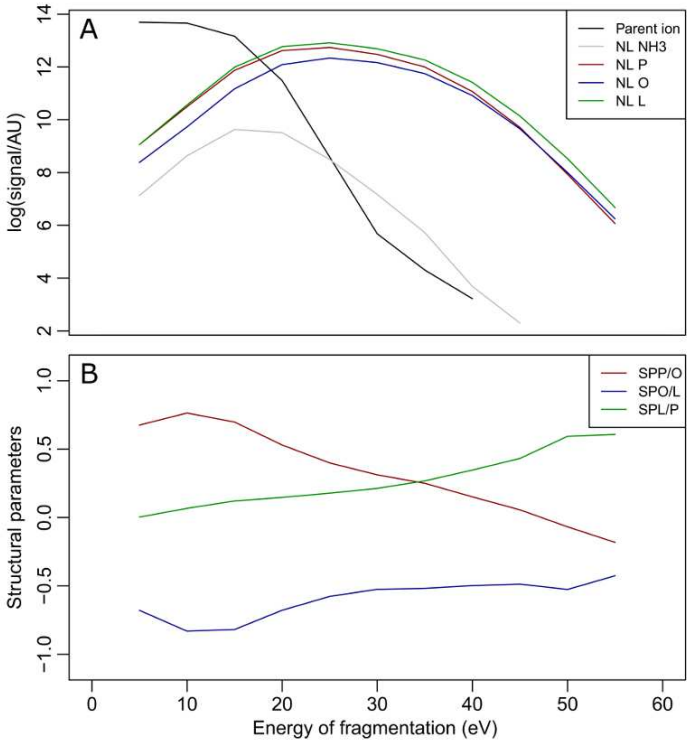
A
Parent ion
NL NH3
NL P
NL O
NL L
log(signal/AU)
2
4
6
8
10
12
14
B
SPP/O
SPO/L
SPL/P
Structural parameters
−1.0
−0.5
0.0
0.5
1.0
0
10
20
30
40
50
60
Energy of fragmentation (eV)

Figure 3

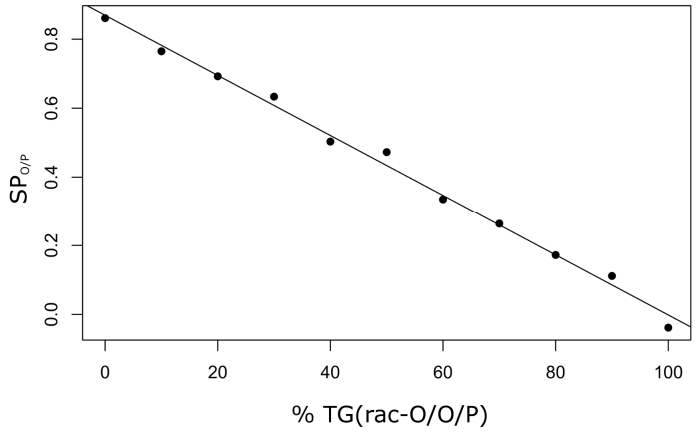

Table 1. Calibration bias of the multivariate constrained regression. The bias of quantified regioisomeric composition is expressed as the average of the absolute value of the deviation of the quantified value. The regression matrix was fitted by: A) minimizing the sum of squares of the measured structural parameters in every type of mixture, B) interpolation among the average of extremes (pure regioisomers), and C) by using the modeled structural vectors as columns in the regression matrix. The data were acquired in the same conditions as the Boston dataset. In all cases the parent ion of the fragmentations was the adduct $[M+NH_4]^+$.

Table 2. Fragmentation parameters (γ) fitted for the different datasets.

Table 3. Efficiency of the fragmentation of the TGs depending on the number of carbons and unsaturations. The efficiency of fragmentation was quantified as the sum of the signal of the neutral losses of the fatty acids divided by the signal of the parent ion ($\Sigma NL/[M+NH_4]^+$). The experiments were carried out on a Synapt G2S Q-ToF in Nantes at 13 V of fragmentation energy. C and U stand, respectively, for the total number of acyl carbons and unsaturation in the TG.

Table 4. Comparison of the quantification of the regioisomeric composition of TGs in sunflower and olive oils with previously reported results. The regioisomers of TGs were quantified by the prediction of the fragmentation patterns by the parameters in Table 2 for the Nantes dataset. The regioisomers that were not present in this dataset are in marked with an asterisk.

Table 1

Regression matrix	Calibration Bias (%)		
	Minimum sum of squares	Interpolation between average of extremes	Modeled fragmentation patterns
TG(rac-O/S/O) TG(rac-S/O/O)	2.9	5.0	9.5
TG(rac-S/O/S) TG(rac-S/S/O)	2.1	4.1	8.7
TG(rac-P/S/O) TG(rac-S/P/O) TG(rac-P/O/S)	3.1	3.9	3.0

Table 2

		ESI, $[M+NH_4]^+$ CID fragmentation		**APCI, $[M+H]^+$ Spontaneous fragmentation**				
	Dataset	Boston	Nantes	Pardubice				
	Instrument	Ion-trap	Q-ToF	Orbitrap	Q-ToF	Ion-trap	SQ	TQ
Position	γ_{int}	0	0	0	0	0	0	0
	γ_{ext}	-0.96	-0.65	-0.66	-0.65	-0.64	-0.70	-0.67
Type of fatty acid	γ_{sat}	0	0	0	0	0	0	0
	γ_{MU}	-0.21	-0.28	-0.0026	-0.050	0.014	-0.047	-0.018
	γ_{L}	-0.32	-0.20	-0.22	-0.30	-0.11	-0.29	-0.18
	γ_{ALA}	-0.59	-0.22	-0.20	-0.16	-0.081	-0.17	-0.14
	γ_{GLA}	-1.45	-0.82	-1.30	-1.14	-1.10	-1.27	-1.14
	γ_{AA}	-2.16	NA*	NA	NA	NA	NA	NA
	γ_{EPA}	-1.86	NA	NA	NA	NA	NA	NA
	γ_{DHA}	-3.15	NA	NA	NA	NA	NA	NA
Interaction	γ_{IN}	1.31	0.27	0.39	0.32	0.43	0.36	0.48

*NA, non-applicable because the fatty acid was not available in the dataset

Table 3

TG(C:U)	TG	Efficiency of fragmentation
TG(50:1)	TG(rac-P/O/P)	$9.47\ 10^{-04}$
	TG(rac-P/P/O)	$8.11\ 10^{-04}$
TG(50:2)	TG(rac-P/L/P)	$8.19\ 10^{-04}$
TG(52:1)	TG(rac-S/P/O)	$7.42\ 10^{-04}$
TG(52:2)	TG(rac-O/P/O)	$7.95\ 10^{-04}$
	TG(rac-O/O/P)	$7.42\ 10^{-04}$
TG(52:2)	TG(rac-P/L/S)	$6.72\ 10^{-04}$
TG(52:3)	TG(rac-P/O/L)	$5.56\ 10^{-04}$
TG(52:4)	TG(rac-L/L/P)	$3.56\ 10^{-04}$
TG(54:1)	TG(rac-M/O/B)	$6.53\ 10^{-04}$
TG(54:4)	TG(rac-O/L/O)	$5.28\ 10^{-04}$
	TG(rac-O/O/L)	$4.34\ 10^{-04}$
TG(54:4)	TG(rac-L/S/L)	$3.54\ 10^{-04}$
TG(54:5)	TG(rac-L/O/L)	$3.21\ 10^{-04}$
	TG(rac-L/L/O)	$3.05\ 10^{-04}$
TG(54:5)	TG(rac-O/O/ALA)	$3.20\ 10^{-04}$
TG(54:7)	TG(rac-L/L/GLA)	$2.13\ 10^{-04}$

Table 4

		Sunflower seed oil		Olive oil	
	Regioisomer	Quantified	Bibliography	Quantified	Bibliography
TG(50:1)	TG(rac-P/O/P)	100	100 [11]; 100 [42]	100	97 [22]; 98 [43]
	TG(rac-P/P/O)	0	0 [11]; 0 [42]	0	3 [22]; 2 [43]
TG(50:2)	TG(rac-P/L/P)	91	100 [11]; 100 [42]	88	-
	TG(rac-P/P/L)*	9	0 [11]; 0 [42]	13	
TG(52:1)	TG(rac-P/S/O)*	0	0 [11]	0	-5[¥] [31]
	TG(rac-P/O/S)*	100	100 [11]	100	105 [31]
	TG(rac-S/P/O)	0	0 [11]	0	8 [31]
TG(52:2)	TG(rac-O/P/O)	0	0 [11]; 2 [42]; 9 [44]	0	2 [22]; 5 [43]
	TG(rac-O/O/P)	100	100 [11]; 98 [42]; 91 [44]	100	98 [22]; 95 [43]
TG(52:2)	TG(rac-P/S/L)*	21	0 [11]	-	-
	TG(rac-P/L/S)	71	100 [11]		
	TG(rac-S/P/L)*	9	0 [11]		
TG(52:3)	TG(rac-P/O/L)	52	45 [11]; 36 [42]	47	-
	TG(rac-P/L/O)*	48	55 [11]; 63 [42]	53	
	TG(rac-O/P/L)*	0	0 [11]; 1 [42]	0	
TG(52:4)	TG(rac-L/P/L)*	0	3 [42]	20	26 [43]
	TG(rac-L/L/P)	100	97 [42]	80	74 [43]
TG(54:2)	TG(rac-O/S/O)*	0	0 [11]	0	6 [43]; -5[¥] [31]
	TG(rac-O/O/S)*	100	100 [11]	100	94 [43]; 105 [31]
TG(54:2)	TG(rac-S/L/S)*	35[§]	100 [11]	0[§]	-
	TG(rac-S/S/L)*	65[§]	0 [11]	100[§]	
TG(54:3)	TG(rac-S/O/L)*	42	45 [11]	26	-
	TG(rac-S/L/O)*	58	55 [11]	74	
	TG(rac-O/S/L)*	0	0 [11]	0	
TG(54:4)	TG(rac-O/L/O)	41	38 [11]; 39 [45]	62	49 [22]; 39 [43]
	TG(rac-O/O/L)	59	62 [11]; 61 [45]	38	51 [22]; 61 [43]
TG(54:4)	TG(rac-L/S/L)	1	0 [11]	17	-
	TG(rac-L/L/S)*	99	100 [11]	83	
TG(54:5)	TG(rac-L/O/L)	47	29 [11]; 27 [44]; 7 [45]	26	15 [22]; 33 [43]; 0 [44]
	TG(rac-L/L/O)	53	71 [11]; 73 [44]; 93 [45]	74	85 [22]; 67 [43]; 100 [44]

[§]Minor component

[¥]Negative values correspond to external quantifications without constrained calibration

Equations

$$SP_{A/B} = \ln\left(\frac{I_A/M_A}{I_B/M_B}\right) = \ln\left(\frac{I_A}{I_B}\right) - \ln\left(\frac{M_A}{M_B}\right) \ (Equation\ 1)$$

$$SV_{TG(A/B/C)} = \begin{pmatrix} SP_{A/B,TG(A/B/C)} \\ SP_{B/C,TG(A/B/C)} \\ SP_{C/A,TG(A/B/C)} \end{pmatrix} (Equation\ 2)$$

$$SV_{mixture} = \sum_i \alpha_i * SV_i \ ; constrains \begin{cases} \sum_i \alpha_i = 1 \\ 0 \leq \alpha_i \ \leq 1, \forall\ i\ (regioisomer) \end{cases} (Equation\ 3)$$

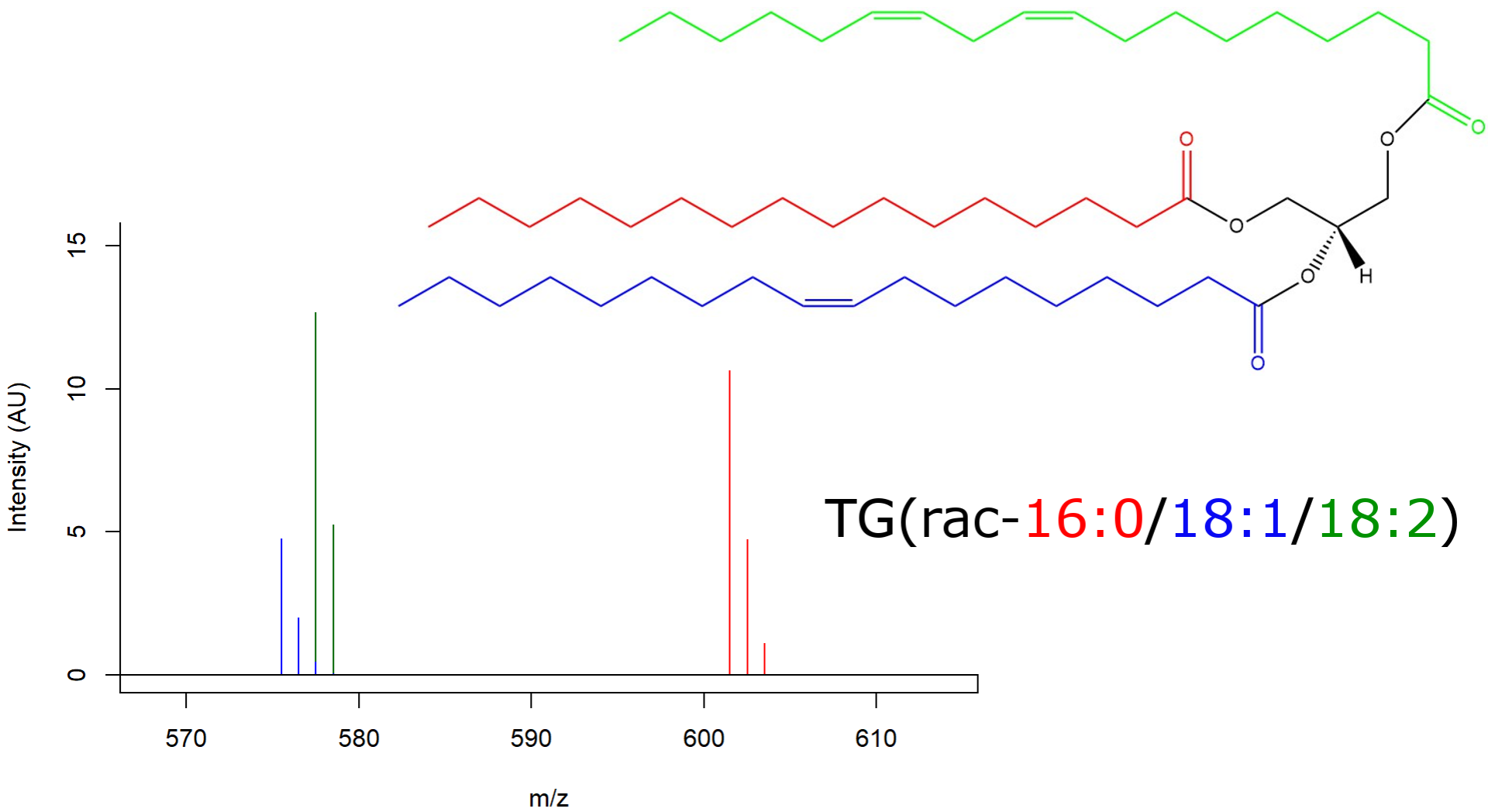
Intensity (AU)
0
5
10
15
570
580
590
600
610
m/z
O
O
O
O
O
O
H
TG(rac-16:0/18:1/18:2)